THE JOURNAL OF PHYSICAL CHEMISTRY LETTERS
A JOURNAL OF THE AMERICAN CHEMICAL SOCIETY

pubs.acs.org/JPCL Letter

Acquisition of ^{1}H-Detected ^{103}Rh and ^{99}Ru Solid-State Nuclear Magnetic Resonance Spectra in Stationary Samples

James J. Kimball and Robert W. Schurko*

Cite This: J. Phys. Chem. Lett. 2025, 16, 4596−4601 Read Online

ACCESS | Metrics & More | Article Recommendations | Supporting Information

ABSTRACT: The platinum group elements (PGEs) are among the most important in the periodic table due to their critical roles in a diverse array of applications. There is great interest in using solid-state nuclear magnetic resonance (SSNMR) for studying the structure and bonding in PGE complexes from the perspective of the metal nuclides, yet this has been limited to date. This is largely due to the inherently low Larmor frequencies of many of the PGE nuclides in addition to factors such as low natural abundances and/or large anisotropic interactions that reduce their receptivity to the NMR experiment. In this work, we demonstrate for the first time the ability to indirectly detect (with ^{1}H, I = 1/2) wideline SSNMR powder patterns from stationary samples of compounds featuring ^{103}Rh (S = 1/2) and ^{99}Ru (S = 5/2) using the recently introduced progressive saturation of the proton reservoir (PROSPR) pulse sequence.

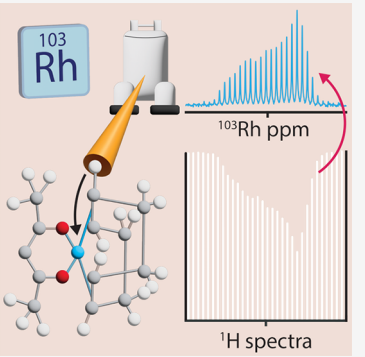

The platinum group elements (PGEs), which include ruthenium, rhodium, palladium, iridium, osmium, and platinum, play essential roles in modern technologies, such as catalysis, electronics, and industrial chemical processes.[1−3] However, exorbitant prices and widespread scarcity of the PGEs have fueled an ongoing search for so-called replacement metals, which would serve to address issues of cost, supply, and sustainability.[4] However, many of the useful properties of PGE complexes emerge from their unique chemical bonds with a wide assortment of ligands; as such, it is necessary to investigate the nature of these ill-understood bonding interactions, which would aid in the discovery of replacement metals and novel ligands that may be combined to mimic the properties and emergent functions of PGE complexes.

Solid-state nuclear magnetic resonance (SSNMR) spectroscopy, in combination with first-principles density functional theory (DFT) calculations, represents a premier method for the investigation of structure and bonding in transition metal complexes.[5−12] However, SSNMR investigations of the PGEs are uncommon, with the exception of ^{195}Pt SSNMR studies of an abundance of materials and compounds.[13−17] To date, there are only a handful of papers describing applications of ^{99}Ru, ^{103}Rh, and ^{105}Pd SSNMR to chemical compounds,[18−24] and no similar reports of $^{187/189}$Os or $^{191/193}$Ir SSNMR. This is largely due to the unreceptivity of these PGE nuclides to the NMR experiment, which arises from their low gyromagnetic ratios (γ), low natural abundances (n.a.), and/or large anisotropic interactions.[25−27] Such properties make NMR experimentation formidable due in part to the long time periods required to obtain spectra with high signal-to-noise ratios (SNRs).

Cross-polarization (CP) is one of the most widely used techniques in NMR and is aimed directly at mitigating the issue of low SNRs.[10,28−30] CP employs radio frequency (RF) pulses to achieve a set of experimental conditions in which the Hartmann−Hahn (HH) matching conditions are fulfilled, thereby establishing thermal contact between abundant spins (most commonly ^{1}H, referred to herein as I spins) and dilute spins (referred to herein as S spins).[31] The exact form of the HH matching conditions depends on the type of field along which the spin polarization of the abundant spins is quantized. A state of Zeeman order (ZO) is one in which the I spins are quantized along the externally applied magnetic field ($\mathbf{B}_0$), and upon transformation of ZO into the rotating frame, the HH match can be fulfilled by the application of simultaneous spin locking pulses on the I and S channels (SL-CP).[32,33] A state of dipolar order (DO) is one wherein the I spin polarization is quantized along local internal fields arising from the internuclear dipolar interactions,[34−37] and the HH match can be fulfilled by application of a spin lock pulse applied to the S channel only (DO-CP).[38,39]

The effects of CP can be observed either through direct detection (DD), wherein the enhanced signals of the S spin are measured,[40−42] or through indirect detection (ID), wherein the acquisition of the I spin spectrum is used to detect the enhanced S spin polarization. While DD is more commonly used due to its capability in providing superior spectral

Received: February 5, 2025
Revised: April 13, 2025
Accepted: April 16, 2025
Published: May 1, 2025

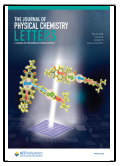

https://doi.org/10.1021/acs.jpclett.5c00378
J. Phys. Chem. Lett. 2025, 16, 4596−4601

resolution and oftentimes faster acquisition times, ID methods, such as dipolar-driven variations of heteronuclear multiple quantum correlation (HMQC) and insensitive nuclei enhancement by polarization transfer (INEPT), can provide increased SNRs and additional information on internuclear proximity, thereby making them advantageous in applications requiring maximal sensitivity.[43−49] ID techniques are commonplace under magic angle spinning (MAS), yet there are only several reports of its use for the acquisition of spectra under static conditions (also referred to as non-rotating or stationary sample conditions),[50,51] despite the advantages that such experiments might offer. These include more precise determination of NMR interaction tensor parameters, the ability to study oriented samples, compatibility with low-temperature conditions, and simplified experimental setups. Additionally, stationary conditions accommodate a wider range of samples for which MAS is impractical or unfeasible.

Jaroszewicz and co-workers recently introduced the progressive saturation of the proton reservoir (PROSPR) sequence (Scheme 1) that makes use of both DO-CP and ID

Scheme 1. Schematic Representation of the PROSPR Pulse Sequence

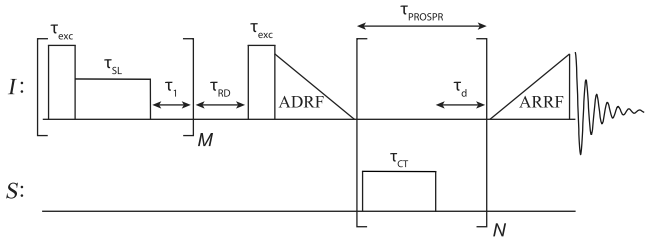

for the acquisition of static SSNMR spectra.[52] Analogous to the chemical exchange saturation transfer (CEST) experiment,[53] PROSPR relies on the depletion of the signal of an abundant nucleus (usually ^{1}H) to indirectly map out the spectrum of a dilute S spin.[54,55] Following presaturation of the I-spin magnetization, a recycle delay of sufficient length, and creation of DO, polarization is transferred during the contact time (τ_{CT}) from the proximate, heteronuclear-coupled protons to the S spins upon fulfilment of the DO-CP HH match using a low-power RF pulse ($\nu_{1,S}$). The subsequent delay period (τ_d) allows for polarization from more distant protons, which are not dipolar coupled to the S spins, to be transferred via spin diffusion to repolarize the neighboring protons, thereby replenishing the large ^{1}H spin polarization bath for subsequent rounds of transfer to the S spins. Simultaneously occurring during τ_d is the decoherence of the accumulated S spin signal via $T_2(S)$, a process that resets the relative spin temperature of the I and S spin baths in a manner favorable for CP. This cycle is repeated as many times as is permitted by the lifetime of the DO [as given by the relaxation time constant of the DO state, $T_{1D}(I)$]. For low-γ nuclei, efficient polarization transfer requires the total length of this cycle [$\tau_{PROPSR} = (\tau_{CT} + \tau_d) \times N$] to be several hundred milliseconds. The powder pattern of the S spin can be mapped out by variation of the transmitter offset frequency of the contact pulse (Ω_S) and observation of the corresponding ^{1}H signal depletion.

The goal of this work is to present a preliminary demonstration of the use of PROPSR for the efficient acquisition of static SSNMR spectra of two unreceptive PGE nuclides: ^{103}Rh (S = 1/2) and ^{99}Ru (S = 5/2). A comparison is made between spectra acquired with PROSPR and the broadband adiabatic inversion-CP/WURST-CPMG pulse sequence (BRAIN-CP/WCPMG), the current state-of-the-art method for the direct detection of CP-enhanced wideline and ultra-wideline (UW) powder patterns under static conditions.[56−59] Consideration is given to the SNR, resolution, and experimental times required for the acquisition of spectra with both methods. Details concerning experimental implementation and spectral processing are provided in Supplements S1 and S2 of the Supplementary Information.

^{103}Rh (S = 1/2) is the second most receptive PGE nuclide due to its 100% natural abundance, despite its low gyromagnetic ratio and potentially large chemical shift anisotropy (CSA). ^{1}H spectra of Rh(COD)(acac) acquired using PROSPR are plotted as a function of Ω_S (Figure 1),

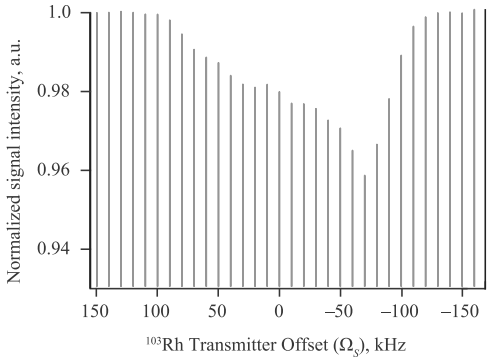

Figure 1. ^{1}H NMR spectra of Rh(COD)(acac) acquired at 18.8 T by using PROSPR.

tracing out a characteristic rhodium CSA pattern that reflects the ^{103}Rh SSNMR powder pattern. Spectral processing (see Supplement S2 for details) allows for an alternative, more conventional presentation of the spectrum (Figure 2a). A comparison to the spectrum acquired with BRAIN-CP/

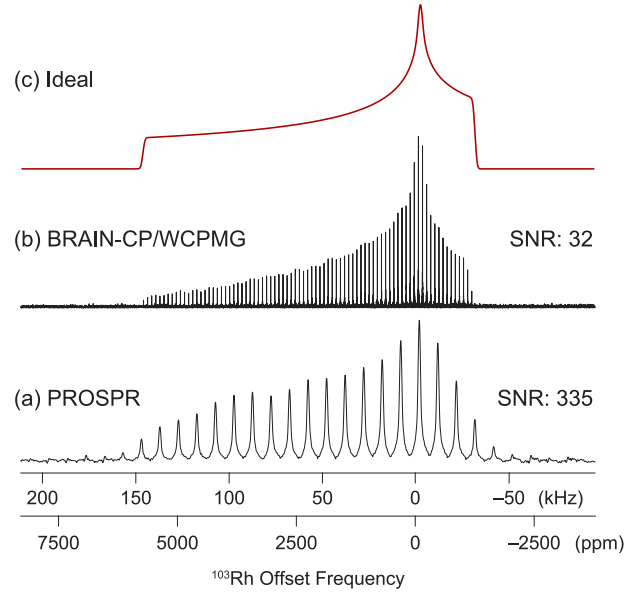

Figure 2. (a and b) ^{1}H−^{103}Rh NMR spectra of Rh(COD)(acac) acquired at (a) 18.8 T using PROSPR (47 min) and (b) 21.1 T using BRAIN-CP/WCPMG (5.6 h). (c) Ideal ^{103}Rh spectrum of Rh(COD)(acac).

https://doi.org/10.1021/acs.jpclett.5c00378
J. Phys. Chem. Lett. 2025, 16, 4596−4601

WCPMG (Figure 2b, as presented in a previous work[23]) and the ideal simulation (Figure 2c) confirms that PROSPR is successful in producing a powder pattern with the appropriate distinctive features (i.e., pattern breadth and key discontinuities). PROSPR allows for the use of significantly lower ^{103}Rh RF powers on the S channel (6 kHz vs 20 kHz for BRAIN-CP; see Tables S1 and S2 for experimental details), reduces experimental time (47 min vs 5.6 h), and delivers an order of magnitude gain in SNR. However, the resolution of the PROSPR spectrum is clearly inferior to that observed in the BRAIN-CP/WCPMG spectrum, in part, due to the S transmitter step size ($\Delta\Omega_S$ = 10 kHz), which was chosen to maximally accelerate the experiment. Nonetheless, the CS tensor parameters determined from the PROSPR spectrum (Table 1) are in good agreement with those reported by Holmes et al.,[23] albeit with higher uncertainties. It is important to note that, in the event that PROSPR is not capable of providing the desired level of spectral resolution, it is still worthwhile to consider its use for preliminary experiments, wherein a broad powder pattern dominated by CSA can quickly be identified and mapped out and the principal components of the CS tensor can be easily measured, thereby providing valuable insight for further spectral acquisition of higher resolution powder patterns.

Table 1. Best Fit ^{103}Rh CS Tensor Parameters Are from Figure 2a and b[a,b]

method	δ_{iso} (ppm)	Ω_{CS} (ppm)	κ
BRAIN-CP/WCPMG[23]	1280(50)	7030(120)	−0.67(0.03)
PROSPR (this work)	1340(60)	7220(300)	−0.66(0.04)

[a]CS tensors are reported using the Herzfeld−Berger convention. [b]Uncertainties in the CS parameters are given in parentheses; e.g., 1280 ± 50 = 1280(50).

Quantitative comparison of spectra acquired using DD and ID methods can be nuanced due in part to the origin of the spikelet spacing in each type of experiment. CPMG-type experiments used for DD of spectra featuring wideline and UWNMR powder patterns result in spikelet spacing that is typically at the control of the experimentalist but dependent upon both the effective T_2, T_2^{eff}, and even the types of pulses used (i.e., rectangular or frequency swept).[60,61] CPMG experiments involving low-γ nuclei oftentimes necessitate lengthy dead times in order to avoid the deleterious effects of acoustic ringing;[62] thus, the resulting frequency domain spectra frequently feature closely spaced spikelets. The spikelet spacing in PROSPR experiments is determined by $\Delta\Omega_S$ (see Supplement S2.1). In principle, the spectral resolution is determined by the amplitude of the contact pulse, $\nu_{1,S}$, which controls the CP bandwidth, yet homonuclear dipolar couplings oftentimes result in a broadening of the matching conditions. Thus, the resolution of a powder pattern from an ID PROSPR spectrum acquired with a given $\nu_{1,S}$ is oftentimes lower than that of a DD BRAIN-CP/WCPMG spectrum.

^{99}Ru SSNMR is significantly more challenging, largely due to its lower natural abundance (i.e., 12.76% for ^{99}Ru vs. 100% for ^{103}Rh). The larger gyromagnetic ratio of ^{99}Ru [i.e., $\gamma(^{99}\text{Ru})/\gamma(^{103}\text{Rh})$ = 1.445] offers some benefits; however, because ^{99}Ru is a quadrupolar nuclide (I = 5/2), experiments can be complicated by the complex nutation behavior of the isochromats in its central transition (CT, +1/2 ↔ −1/2) powder pattern and its satellite transitions (±1/2 ↔ ±3/2 and ±3/2 ↔ ±5/2) as well as CSA effects and well-known issues with CP between spin-1/2 and quadrupolar nuclides.[64−67]

The ^{99}Ru spectra of (2-MeAl)$_2$Ru(COD) acquired at 18.8 T with PROSPR (Figure 3a) and BRAIN-CP (Figure 3b) are compared to the ideal simulation (Figure 3c). The breadth of the powder pattern is well-represented in both cases, but discontinuities in the central region of the PROSPR pattern are ill-defined, reinforcing the challenges associated with SSNMR spectroscopy of unreceptive nuclides like ^{99}Ru. As neither the ^{99}Ru EFG tensor parameters nor the crystal structure of (2-MeAl)$_2$Ru(COD) have previously been reported, the best fit parameters from the BRAIN-CP spectrum (Table 2) are used to simulate the ideal powder pattern (N.B.: the absence of spectral acquisition at a second field reduces the accuracy of the fit). Both experimental spectra share similar SNR (as best as can be measured) and resolution as the PROSPR spectrum is acquired with transmitter step sizes of $\Delta\Omega_S$ = 5 kHz. The single-channel RF power requirements for PROSPR ($\nu_{1,S} \approx 5$ kHz) represent an attractive alternative to the double-resonance requirements for BRAIN-CP/WCPMG ($\nu_{1,S} \approx 11$ kHz and $\nu_{1,I} \approx 30$ kHz), albeit with resulting spectra of decreased quality. While PROSPR is successful at tracing out the ^{99}Ru powder pattern, BRAIN-CP/WCPMG currently represents a more robust method for the precise measurement of the CS and EFG tensor parameters in this case. Further explorations of ^{1}H−^{99}Ru PROSPR NMR and its optimization are underway.

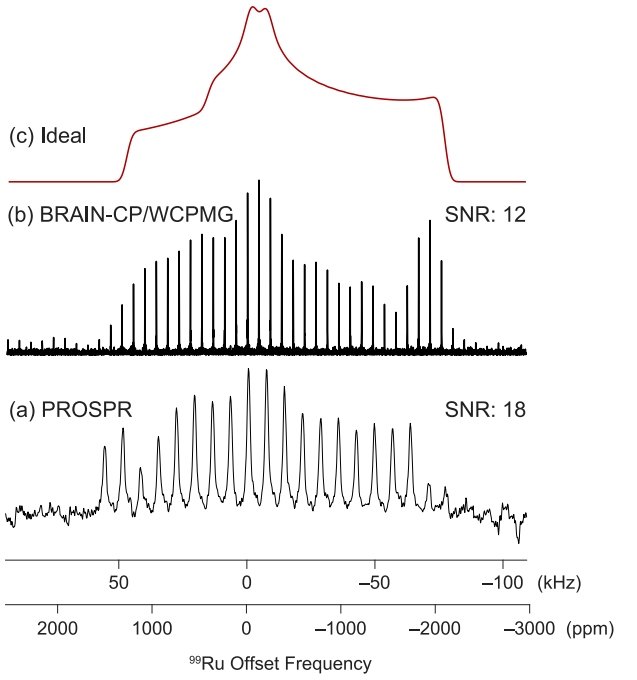

Figure 3. (a and b) ^{1}H−^{99}Ru NMR spectra of (2-MeAl)$_2$Ru(COD) acquired at 18.8 T using (a) PROSPR (1.4 h) and (b) BRAIN-CP/WCPMG (4.3 h). (c) Ideal ^{99}Ru NMR spectrum of (2-MeAl)$_2$Ru(COD).

The spectral quality (as determined by the SNR and the experimental length) of the PROSPR spectrum of (2-MeAl)$_2$Ru(COD) (Figure 3a) is lower than that of Rh(COD)(acac) (Figure 2b) despite the longer $T_{1D}(I)$ of the former [ca. $T_{1D}(I)$ = 1.5 and 0.9 s, respectively; see Figure S2]. This discrepancy is likely due to much lower n.a. of ^{99}Ru, which

https://doi.org/10.1021/acs.jpclett.5c00378
J. Phys. Chem. Lett. 2025, 16, 4596−4601

Table 2. Best Fit ^{99}Ru CS and EFG Tensor Parameters Are from Figure 3b[a]

δ_{iso} (ppm)	Ω_{CS} (ppm)	κ	C_Q (MHz)	η_Q	φ (deg)	χ (deg)	ψ (deg)
−170(20)	2450(50)	−0.65(0.05)	9.9(0.2)	0.05(0.05)	170(10)	50(5)	100(20)

[a]CS tensors are reported using the Herzfeld−Berger convention. Euler angles are related to the conventional angles α, β, and γ by $\varphi = -\arccos(\cos\beta/\sin\chi)$, $\chi = -\arccos(-\sin\beta\cos\gamma)$, and $\psi = -\arcsin(-(\sin\alpha\cos\beta\cos\gamma + \cos\alpha + \sin\gamma)/\sin\chi) + 90°$.[63]

limits the number of pathways for polarization transfer and, thus, results in lower ^{1}H signal depletion (Figure S5). Thus, future targets for spectral acquisition via PROSPR, such as ^{57}Fe (n.a. = 2.12%) or ^{17}O (n.a. = 0.038%), represent more challenging cases; however, these could benefit greatly from isotopic enrichment, which is possible for the former and becoming increasingly more routine for the latter.[68]

In summary, we have demonstrated that PROSPR can be used for the indirect detection of spectra of samples under stationary conditions with powder patterns inhomogeneously broadened by both the CS and quadrupolar interactions. Our results suggest that PROSPR is particularly well-suited for applications to low-γ nuclei due to its significantly lower RF requirements and avoidance of simultaneous double-resonance conditions. Even in cases where PROSPR fails to result in significant SNR gains, the RF power considerations alone deem it valuable, as the simultaneous application of high RF fields on two channels as is required in more conventional CP experiments is not an option on many probes and/or can lead to arcing and significant reduction of probe lifetimes. In general, PROSPR is successful in reducing experimental lengths and offers the potential for significant gains in SNR, despite offering decreased spectral resolution relative to analogous DD methods.

The ability to rapidly map out powder patterns of low-γ nuclei serves as convincing evidence that PROSPR is a useful tool for the spectroscopist concerned with the acquisition of wideline and UW NMR spectra. Nevertheless, its signal enhancement capabilities can only be exploited in the limit of $T_{1D}(I)$ values of sufficient length (e.g., several hundred milliseconds or longer). Unfortunately, short proton $T_{1D}(I)$ values are relatively common; hence, PROSPR in its current form is system-dependent. Future work will focus on understanding factors influencing $T_{1D}(I)$, improving the efficiency of DO creation, and leveraging the use of variable temperatures.

We anticipate that a forthcoming study of the setup and optimization of the PROSPR sequence will enable more widespread use of this method for the acquisition of static wideline and UW SSNMR spectra. Increased accessibility to ^{103}Rh and ^{99}Ru SSNMR spectroscopy, in combination with DFT geometry optimizations and concomitant calculations of NMR interaction tensor parameters, will help advance our understanding of PGE bonding and inform strategies for identifying alternative materials to reduce our dependency on these scarce elements.

■ ASSOCIATED CONTENT

Supporting Information

The Supporting Information is available free of charge at https://pubs.acs.org/doi/10.1021/acs.jpclett.5c00378.

Experimental protocols and implementation, spectral processing, and relaxation data (PDF)

■ AUTHOR INFORMATION

Corresponding Author

Robert W. Schurko − *Department of Chemistry & Biochemistry, Florida State University, Tallahassee, Florida 32306, United States; National High Magnetic Field Laboratory, Tallahassee, Florida 32310, United States;* orcid.org/0000-0002-5093-400X; Email: rschurko@fsu.edu

Author

James J. Kimball − *Department of Chemistry & Biochemistry, Florida State University, Tallahassee, Florida 32306, United States; National High Magnetic Field Laboratory, Tallahassee, Florida 32310, United States;* orcid.org/0000-0002-4993-6892

Complete contact information is available at: https://pubs.acs.org/10.1021/acs.jpclett.5c00378

Notes

The authors declare no competing financial interest.

■ ACKNOWLEDGMENTS

James J. Kimball and Robert W. Schurko thank the Basic Energy Sciences Program in the Department of Energy (DE-SC0022310) for supporting this work. They also thank the National Science Foundation Chemical Measurement and Imaging Program, with partial co-funding from the Solid State and Materials Chemistry Program (NSF-2003854), for funding early stages of this work. The National High Magnetic Field Laboratory (NHMFL) is supported by the National Science Foundation (NSF/DMR-1644779 and NSF/DMR-2128556) and the State of Florida. James J. Kimball and Robert W. Schurko thank Lucio Frydman (Weizmann Institute), Mike Jaroszewicz (University of Michigan), Frederic Mentink-Vigier (NHMFL), and Zhehong Gan (NHMFL) for helpful discussions related to theory and spin dynamics. Jason Kitchen and Peter Gor'kov (NHMFL) are thanked for providing the probe modifications necessary for these experiments, which is supported in part by the National Resource for Advanced NMR Technology (RM1 GM148766).

■ REFERENCES

(1) Zientek, M. L.; Loferski, P. J.; Parks, H. L.; Schulte, R. F.; Seal, R. R., II Chapter N. Platinum-Group Elements. In *Critical Mineral Resources of the United States—Economic and Environmental Geology and Prospects for Future Supply*; Schulz, K. J., DeYoung, J. H., Jr., Seal, R. R., II, Bradley, D. C., Eds.; U.S. Geological Survey: Reston, VA, 2017; Professional Paper 1802, DOI: 10.3133/pp1802.

(2) Hughes, A. E.; Haque, N.; Northey, S. A.; Giddey, S. Platinum group metals: A review of resources, production and usage with a focus on catalysts. *Resources* **2021**, *10*, 93.

(3) Sinisalo, P.; Lundström, M. Refining Approaches in the Platinum Group Metal Processing Value Chain—A Review. *Metals* **2018**, *8*, 203.

(4) Nassar, N. T. Limitations to elemental substitution as exemplified by the platinum-group metals. *Green Chem.* **2015**, *17*, 2226.

(5) Wasylishen, R. E.; Bernard, G. M. Solid-state NMR spectroscopy in organometallic chemistry. In *Comprehensive Organometallic Chemistry III*; Elsevier, Ltd.: Amsterdam, Netherlands, 2007; Vol. *1*, pp 451−482, DOI: 10.1016/B0-08-045047-4/00019-4.
(6) Foucault, H. M.; Bryce, D. L.; Fogg, D. E. A chelate-stabilized ruthenium (σ-pyrrolato) complex: Resolving ambiguities in nuclearity and coordination geometry through ^{1}H PGSE and ^{31}P solid-state NMR studies. *Inorg. Chem.* **2006**, *45*, 10293.
(7) Autschbach, J.; Zheng, S. Analyzing Pt chemical shifts calculated from relativistic density functional theory using localized orbitals: The role of Pt 5d lone pairs. *Magn. Reson. Chem.* **2008**, *46*, S45.
(8) Johnston, K. E.; O'Keefe, C. A.; Gauvin, R. M.; Trébosc, J.; Delevoye, L.; Amoureux, J.-P.; Popoff, N.; Taoufik, M.; Oudatchin, K.; Schurko, R. W. A Study of Transition-Metal Organometallic Complexes Combining 35 Cl Solid-State NMR Spectroscopy and 35 Cl NQR Spectroscopy and First-Principles DFT Calculations. *Chem. - Eur. J.* **2013**, *19*, 12396.
(9) O'Keefe, C. A.; Johnston, K. E.; Sutter, K.; Autschbach, J.; Gauvin, R.; Trébosc, J.; Delevoye, L.; Popoff, N.; Taoufik, M.; Oudatchin, K.; et al. An Investigation of Chlorine Ligands in Transition-Metal Complexes via 35 Cl Solid-State NMR and Density Functional Theory Calculations. *Inorg. Chem.* **2014**, *53*, 9581.
(10) Smith, M. E. Recent progress in solid-state NMR of spin-1/2 low-γ nuclei applied to inorganic materials. *Phys. Chem. Chem. Phys.* **2022**, *25*, 26.
(11) Gordon, C. P.; Lätsch, L.; Copéret, C. Nuclear Magnetic Resonance: A Spectroscopic Probe to Understand the Electronic Structure and Reactivity of Molecules and Materials. *J. Phys. Chem. Lett.* **2021**, *12*, 2072.
(12) Grekov, D.; Vancompernolle, T.; Taoufik, M.; Delevoye, L.; Gauvin, R. M. Solid-state NMR of quadrupolar nuclei for investigations into supported organometallic catalysts: Scope and frontiers. *Chem. Soc. Rev.* **2018**, *47*, 2572.
(13) Still, B. M.; Kumar, P. G. A.; Aldrich-Wright, J. R.; Price, W. S. ^{195}Pt NMR—theory and application. *Chem. Soc. Rev.* **2007**, *36*, 665.
(14) Sparks, S. W.; Ellis, P. D. Platinum-195 shielding tensors in potassium hexachloroplatinate(IV) and potassium tetrachloroplatinate(II). *J. Am. Chem. Soc.* **1986**, *108*, 3215.
(15) Rhodes, H. E.; Wang, P.-K.; Stokes, H. T.; Slichter, C. P.; Sinfelt, J. H. NMR of platinum catalysts. I. Line shapes. *Phys. Rev. B* **1982**, *26*, 3559.
(16) Harris, R. K.; Reams, P.; Packer, K. J. High-resolution solid-state platinum-195 nuclear magnetic resonance. *J. Chem. Soc. Dalt. Trans.* **1986**, 1015.
(17) Lucier, B. E. G.; Johnston, K. E.; Xu, W.; Hanson, J. C.; Senanayake, S. D.; Yao, S.; Bourassa, M. W.; Srebro, M.; Autschbach, J.; Schurko, R. W. Unravelling the structure of Magnus' pink salt. *J. Am. Chem. Soc.* **2014**, *136*, 1333.
(18) Phillips, B. L.; Houston, J. R.; Feng, J.; Casey, W. H. Observation of solid-state ^{103}Rh NMR by cross-polarization. *J. Am. Chem. Soc.* **2006**, *128*, 3912.
(19) Ooms, K. J.; Wasylishen, R. E. Solid-state Ru-99 NMR spectroscopy: A useful tool for characterizing prototypal diamagnetic ruthenium compounds. *J. Am. Chem. Soc.* **2004**, *126*, 10972.
(20) Venkatesh, A.; Ryan, M. J.; Biswas, A.; Boteju, K. C.; Sadow, A. D.; Rossini, A. J. Enhancing the Sensitivity of Solid-State NMR Experiments with Very Low Gyromagnetic Ratio Nuclei with Fast Magic Angle Spinning and Proton Detection. *J. Phys. Chem. A* **2018**, *122*, 5635.
(21) Harbor-Collins, H.; Sabba, M.; Moustafa, G.; Legrady, B.; Soundararajan, M.; Leutzsch, M.; Levitt, M. H. The ^{103}Rh NMR spectroscopy and relaxometry of the rhodium formate paddlewheel complex. *J. Chem. Phys.* **2023**, *159*, 104307.
(22) Harbor-Collins, H.; Sabba, M.; Bengs, C.; Moustafa, G.; Leutzsch, M.; Levitt, M. H. NMR spectroscopy of a ^{18}O-labeled rhodium paddlewheel complex: Isotope shifts, ^{103}Rh-^{103}Rh spin-spin coupling, and ^{103}Rh singlet NMR. *J. Chem. Phys.* **2024**, *160*, 14305.
(23) Holmes, S. T.; Schönzart, J.; Philips, A. B.; Kimball, J. J.; Termos, S.; Altenhof, A. R.; Xu, Y.; O'Keefe, C. A.; Autschbach, J.; Schurko, R. W. Structure and bonding in rhodium coordination compounds: a 103 Rh solid-state NMR and relativistic DFT study. *Chem. Sci.* **2024**, *15*, 2181.
(24) Hooper, T. J. N.; Partridge, T. A.; Rees, G. J.; Keeble, D. S.; Powell, N. A.; Smith, M. E.; Mikheenko, I. P.; Macaskie, L. E.; Bishop, P. T.; Hanna, J. V. Direct solid state NMR observation of the ^{105}Pd nucleus in inorganic compounds and palladium metal systems. *Phys. Chem. Chem. Phys.* **2018**, *20*, 26734.
(25) Sebald, A. MAS and CP/MAS NMR of Less Common Spin-1/2 Nuclei. In *Solid-State NMR II*; Blümich, B., Ed.; Springer-Verlag: Berlin, Germany, 1994; NMR Basic Principles and Progress, Vol. *31*, pp 91−131, DOI: 10.1007/978-3-642-50049-7_3.
(26) Schurko, R. W. Acquisition of Wideline Solid-State NMR Spectra of Quadrupolar Nuclei. In *Encyclopedia of Magnetic Resonance*; Harris, R. K., Ed.; John Wiley & Sons, Ltd: Chichester, U.K., 2011; DOI: 10.1002/9780470034590.emrstm1199.
(27) Schurko, R. W. Ultra-Wideline Solid-State NMR Spectroscopy. *Acc. Chem. Res.* **2013**, *46*, 1985.
(28) Smith, M. E. Recent progress in solid-state nuclear magnetic resonance of half-integer spin low- γ quadrupolar nuclei applied to inorganic materials. *Magn. Reson. Chem.* **2021**, *59*, 864.
(29) Gan, Z. Perspectives on high-field and solid-state NMR methods of quadrupole nuclei. *J. Magn. Reson.* **2019**, *306*, 86.
(30) Reif, B.; Ashbrook, S. E.; Emsley, L.; Hong, M. Solid-state NMR spectroscopy. *Nat. Rev. Methods Prim.* **2021**, *1*, 2.
(31) Hartmann, S. R.; Hahn, E. L. Nuclear Double Resonance in the Rotating Frame. *Phys. Rev.* **1962**, *128*, 2042.
(32) Marks, D.; Vega, S. A Theory for Cross-Polarization NMR of Nonspinning and Spinning Samples. *J. Magn. Reson. Ser. A* **1996**, *118*, 157.
(33) Shekar, S. C.; Ramamoorthy, A. The unitary evolution operator for cross-polarization schemes in NMR. *Chem. Phys. Lett.* **2001**, *342*, 127.
(34) Slichter, C. P.; Holton, W. C. Adiabatic demagnetization in a rotating reference system. *Phys. Rev.* **1961**, *122*, 1701.
(35) Anderson, A. G.; Hartmann, S. R. Nuclear Magnetic Resonance in the Demagnetized State. *Phys. Rev.* **1962**, *128*, 2023.
(36) Jeener, J.; Du Bois, R.; Broekaert, P. "Zeeman" and "dipolar" spin temperatures during a strong rf irradiation. *Phys. Rev.* **1965**, *139*, A1959.
(37) Jeener, J.; Broekaert, P. Nuclear magnetic resonance in solids: Thermodynamic effects of a pair of rf pulses. *Phys. Rev.* **1967**, *157*, 232.
(38) Lurie, F. M.; Slichter, C. P. Spin Temperature in Nuclear Double Resonance. *Phys. Rev.* **1964**, *133*, A1108.
(39) Wolf, T.; Jayanthi, S.; Lupulescu, A.; Frydman, L. Cross polarization from dipolar-order under magic angle spinning: The ADRF-CPMAS NMR experiment. *J. Chem. Phys.* **2023**, *159*, 224304.
(40) Pines, A.; Gibby, M. G.; Waugh, J. S. Proton-Enhanced Nuclear Induction Spectroscopy. A Method for High Resolution NMR of Dilute Spins in Solids. *J. Chem. Phys.* **1972**, *56*, 1776.
(41) Pines, A.; Gibby, M. G.; Waugh, J. S. Proton-enhanced NMR of dilute spins in solids. *J. Chem. Phys.* **1973**, *59*, 569.
(42) Pines, A.; Shattuck, T. W. Carbon-13 proton NMR cross-polarization times in solid adamantane. *J. Chem. Phys.* **1974**, *61*, 1255.
(43) Schmidt-Rohr, K.; Saalwächter, K.; Liu, S. F.; Hong, M. High-sensitivity ^{2}H NMR in solids by ^{1}H detection. *J. Am. Chem. Soc.* **2001**, *123*, 7168.
(44) Lafon, O.; Wang, Q.; Hu, B.; Vasconcelos, F.; Trébosc, J.; Cristol, S.; Deng, F.; Amoureux, J.-P. Indirect Detection via Spin-1/2 Nuclei in Solid State NMR Spectroscopy: Application to the Observation of Proximities between Protons and Quadrupolar Nuclei. *J. Phys. Chem. A* **2009**, *113*, 12864.
(45) Cavadini, S.; Vitzthum, V.; Ulzega, S.; Abraham, A.; Bodenhausen, G. Line-narrowing in proton-detected nitrogen-14 NMR. *J. Magn. Reson.* **2010**, *202*, 57.
(46) Trebosc, J.; Hu, B.; Amoureux, J. P.; Gan, Z. Through-space R3-HETCOR experiments between spin-1/2 and half-integer

https://doi.org/10.1021/acs.jpclett.5c00378
J. Phys. Chem. Lett. 2025, 16, 4596−4601

quadrupolar nuclei in solid-state NMR. *J. Magn. Reson.* **2007**, *186*, 220.
(47) Rossini, A. J.; Hanrahan, M. P.; Thuo, M. Rapid acquisition of wideline MAS solid-state NMR spectra with fast MAS, proton detection, and dipolar HMQC pulse sequences. *Phys. Chem. Chem. Phys.* **2016**, *18*, 25284.
(48) Venkatesh, A.; Hanrahan, M. P.; Rossini, A. J. Proton detection of MAS solid-state NMR spectra of half-integer quadrupolar nuclei. *Solid State Nucl. Magn. Reson.* **2017**, *84*, 171.
(49) Shen, M.; Trébosc, J.; Lafon, O.; Gan, Z.; Pourpoint, F.; Hu, B.; Chen, Q.; Amoureux, J.-P. Solid-state NMR indirect detection of nuclei experiencing large anisotropic interactions using spinning sideband-selective pulses. *Solid State Nucl. Magn. Reson.* **2015**, *72*, 104.
(50) Grannell, P. K.; Mansfield, P.; Whitaker, M. A. B. 13C Double-Resonance Fourier-Transform Spectroscopy in Solids. *Phys. Rev. B* **1973**, *8*, 4149.
(51) Jacquinot, J. F.; Wenckebach, W. T.; Goldman, M.; Abragam, A. Polarization and NMR Observation of Ca43 Nuclei in CaF2. *Phys. Rev. Lett.* **1974**, *32*, 1096.
(52) Jaroszewicz, M. J.; Altenhof, A. R.; Schurko, R. W.; Frydman, L. Sensitivity Enhancement by Progressive Saturation of the Proton Reservoir: A Solid-State NMR Analogue of Chemical Exchange Saturation Transfer. *J. Am. Chem. Soc.* **2021**, *143*, 19778.
(53) Ward, K. M.; Aletras, A. H.; Balaban, R. S. A New Class of Contrast Agents for MRI Based on Proton Chemical Exchange Dependent Saturation Transfer (CEST). *J. Magn. Reson.* **2000**, *143*, 79.
(54) Wolf, T.; Eden-Kossoy, A.; Frydman, L. Indirectly detected satellite-transition quadrupolar NMR via progressive saturation of the proton reservoir. *Solid State Nucl. Magn. Reson.* **2023**, *125*, 101862.
(55) Wolf, T.; Goobes, Y.; Frydman, L. Sensitivity Enhancement of Ultra-Wideline NMR by Progressive Saturation of the Proton Reservoir Under Magic-Angle Spinning. *ChemPhysChem* **2024**, *25*, 1455.
(56) Harris, K. J.; Lupulescu, A.; Lucier, B. E. G.; Frydman, L.; Schurko, R. W. Broadband adiabatic inversion pulses for cross polarization in wideline solid-state NMR spectroscopy. *J. Magn. Reson.* **2012**, *224*, 38.
(57) Harris, K. J.; Veinberg, S. L.; Mireault, C. R.; Lupulescu, A.; Frydman, L.; Schurko, R. W. Rapid acquisition of 14N solid-state NMR spectra with broadband cross polarization. *Chem. - Eur. J.* **2013**, *19*, 16469.
(58) Altenhof, A. R.; Wi, S.; Schurko, R. W. Broadband adiabatic inversion cross-polarization to integer-spin nuclei with application to deuterium NMR. *Magn. Reson. Chem.* **2021**, *59*, 1009.
(59) Kimball, J. J.; Altenhof, A. R.; Jaroszewicz, M. J.; Schurko, R. W. Broadband Cross-Polarization to Half-Integer Quadrupolar Nuclei: Wideline Static NMR Spectroscopy. *J. Phys. Chem. A* **2023**, *127*, 9621.
(60) Veinberg, S. L.; Lindquist, A. W.; Jaroszewicz, M. J.; Schurko, R. W. Practical considerations for the acquisition of ultra-wideline 14N NMR spectra. *Solid State Nucl. Magn. Reson.* **2017**, *84*, 45.
(61) Hung, I.; Gan, Z. On the practical aspects of recording wideline QCPMG NMR spectra. *J. Magn. Reson.* **2010**, *204*, 256.
(62) Lipton, A. S.; Sears, J. A.; Ellis, P. D. A General Strategy for the NMR Observation of Half-Integer Quadrupolar Nuclei in Dilute Environments. *J. Magn. Reson.* **2001**, *151*, 48.
(63) Perras, F. A.; Paterson, A. L. Automatic fitting of multiple-field solid-state NMR spectra. *Solid State Nucl. Magn. Reson.* **2024**, *131*, 101935.
(64) Kentgens, A. P. M.; Lemmens, J. J. M.; Geurts, F. M. M.; Veeman, W. S. Two-dimensional solid-state nutation NMR of half-integer quadrupolar nuclei. *J. Magn. Reson.* **1987**, *71*, 62.
(65) Vega, A. J. MAS NMR spin locking of half-integer quadrupolar nuclei. *J. Magn. Reson.* **1992**, *96*, 50.
(66) Ashbrook, S. E.; Wimperis, S. Spin-locking of half-integer quadrupolar nuclei in nuclear magnetic resonance of solids: Creation and evolution of coherences. *J. Chem. Phys.* **2004**, *120*, 2719.
(67) Ashbrook, S. E.; Wimperis, S. Spin-locking of half-integer quadrupolar nuclei in nuclear magnetic resonance of solids: Second-order quadrupolar and resonance offset effects. *J. Chem. Phys.* **2009**, *131*, 194509.
(68) Goldberga, I.; Hung, I.; Sarou-Kanian, V.; Gervais, C.; Gan, Z.; Novák-Špačková, J.; Métro, T.-X.; Leroy, C.; Berthomieu, D.; van der Lee, A.; et al. High-Resolution 17 O Solid-State NMR as a Unique Probe for Investigating Oxalate Binding Modes in Materials: The Case Study of Calcium Oxalate Biominerals. *Inorg. Chem.* **2024**, *63*, 10179.

https://doi.org/10.1021/acs.jpclett.5c00378
J. Phys. Chem. Lett. 2025, 16, 4596−4601